index for an individual plant species confirm the use of stomatal frequencies as proxy indicators of fluctuations in paleoatmospheric CO_2 concentration. Calibration of the stomatal indices against the historical relation between stomatal frequency and CO_2 concentrations (*19*) enables quantification of the late Miocene-Pliocene paleoatmospheric signals (Fig. 3). The relative changes so far observed suggest that the corresponding global CO_2 concentration has fluctuated between values of ~280 and ~370 parts per million by volume (ppmv). Covariation with climatic changes supports a causal relation between the CO_2 regime and temperature in late Miocene to Pliocene times. On the basis of such a relation, present-day low stomatal indices suggest that the presumed climatic effects of the human-induced CO_2 increase are lagging behind the stomatal responses in land plants.

The fossil leaf record is characterized by its generally discontinuous nature. The relatively few samples available in any one sedimentary sequence limit the extent to which detailed patterns of paleoatmospheric change can be reconstructed. However, quantitative stomatal analysis of cuticular remains can be used to test whether regional relative temperatures that are inferred from more continuous palynological records consistently reflect paleoatmospheric change (*20*).

REFERENCES AND NOTES

1. D. Raynaud *et al.*, *Science* **259**, 926 (1993).
2. R. A. Berner, *ibid.* **249**, 1382 (1990); *Am. J. Sci.* **291**, 339 (1991).
3. N. J. Shackleton, *Geophys. Monogr. Am. Geophys. Union* **32**, 412 (1985).
4. T. E. Cerling, *Am. J. Sci.* **291**, 377 (1991); see also V. P. Wright and S. D. Vanstone, *J. Geol. Soc. London* **148**, 945 (1991).
5. For a review of the role of organisms as monitors, recorders, motors, and moderators of paleoatmospheric change, see J. D. Hudson, *J. Geol. Soc. London* **146**, 155 (1989).
6. G. D. Farquhar and T. D. Sharkey [*Annu. Rev. Plant Physiol.* **33**, 317 (1982)] provided a simple expression (the supply function), describing the gaseous diffusion of CO_2 from the atmosphere to the intercellular spaces in the leaf

$$A = g_c(c_a - c_i)$$

where A is the assimilation rate, g_c is the conductance to diffusion of CO_2 (the reciprocal of resistance), and c_a and c_i denote CO_2 concentrations in the atmosphere and in the intercellular leaf spaces, respectively. A commonly recognized effect of rising c_a is a decrease in g_c; see S. P. Long, N. R. Baker, C. A. Raines, *Vegetatio* **104/105**, 33 (1993).
7. Equations describing the relation between ambient CO_2 concentration and stomatal parameters are not yet available. Because stomatal frequency can be neither zero nor infinite, CO_2 changes are likely to take the form of a sigmoid response curve. We estimate that among modern plants, a linear response is confined to CO_2 fluctuations between 200 and 400 ppmv. At lower concentrations, CO_2 uptake occurs under RuP_2 saturation; at higher concentrations, stomatal conductance may still become adjusted through changes in the size of the stomata.
8. F. I. Woodward, *Nature* **327**, 617 (1987).
9. Since the studies by Woodward (*8*), both supporting and conflicting results have been published. Conflicting results may be largely explained by differences in methodology [see D. J. Beerling and W. G. Chaloner, *Holocene* **2**, 71 (1992)]. Responses of stomatal frequency to a changing CO_2 regime are also apparent from experiments simulating altitude-controlled partial pressures of CO_2 [see F. I. Woodward and F. A. Bazzaz, *J. Exp. Bot.* **39**, 1771 (1988)].
10. Cuticular matrices of extant seed plants consist of either cutin (a biopolyester), cutan (a newly found polymethylenic biopolymer), or a mixture of both biopolymers; of these components, only cutan is highly resistant to diagenetic processes [see E. W. Tegelaar, H. Kerp, H. Visscher, P. A. Schenck, J. W. De Leeuw, *Paleobiology* **17**, 133 (1991)].
11. D. J. Beerling, W. G. Chaloner, B. Huntley, A. Pearson, M. J. Tooley, *Global Ecol. Biogeogr. Lett.* **1**, 136 (1991); P. K. Van De Water, S. W. Leavitt, J. L. Betancourt, *Geol. Soc. Am. Abstr. Programs* **23**, 352 (1991); W. M. Kürschner, unpublished data.
12. Through a taxonomic analysis, leaves of the Upper Miocene and Pliocene from the Lower Rhine Embayment that are usually identified as *Q. pseudocastanea* or *Q. roburoides* were found to be fossil representatives of *Q. petraea* (J. Van Der Burgh, in preparation).
13. W. H. Zagwijn and H. Hager [*Meded. Werkgr. Tert. Kwartaire Geol.* **24**, 59 (1987)] placed the Pliocene-Pleistocene boundary at the onset of the first distinctive cold phase in the Northern Hemisphere (2.3 Ma). This date contrasts with the position of the boundary in conventional marine standard chronostratigraphy (1.8 Ma); for arguments in favor of a 2.3-Ma boundary, see W. H. Zagwijn [*Quat. Sci. Rev.* **11**, 583 (1992)].
14. Fossil cuticles were removed from the clay matrix by means of collodium peels and treated with HF and CrO_3. Computer-aided calculation of stomatal indices was performed on stored video images of cuticle preparations. Stomatal index = [stomatal density/(stomatal density + epidermal cell density)] × 100. Mean stomatal indices per data point were calculated on the basis of 15 to 25 counts, with the use of cuticle fragments from three leaves.
15. G. K. Sharma and D. B. Dunn, *Bull. Torrey Bot. Club* **95**, 464 (1968); *Can. J. Bot.* **47**, 1211 (1969).
16. J. Van Der Burgh, *Rev. Palaeobot. Palynol.* **26**, 173 (1978); *ibid.* **40**, 33 (1983); *ibid.* **52**, 299 (1987); *Tertiary Res.* **9**, 181 (1988).
17. J. A. Wolfe, *U.S. Geol. Surv. Prof. Pap. 1106* (1979), p. 1.
18. The experimental evidence by Woodward (*8*) demonstrated that changes in stomatal density were paralleled by changes in the stomatal index.
19. A. Neftel, E. Moor, H. Oeschger, B. Stauffer, *Nature* **315**, 45 (1985); H. Friedli, H. Lotscher, H. Oeschger, H. Siegenthaler, B. Stauffer, *ibid.* **324**, 237 (1986); C. D. Keeling *et al.*, *Geophys. Monogr. Am. Geophys. Union* **55**, 165 (1989); R. T. Watson, H. Rodhe, H. Oeschger, U. Siegenthaler, in *Climate Change: The IPCC Scientific Assessment*, J. T. Houghton, G. J. Jenkins, J. J. Ephraums, Eds. (Cambridge Univ. Press, Cambridge, 1990), p. 9.
20. To test how well climate models predict conditions on a warmer Earth, one must investigate, most notably, the Pliocene for information on CO_2 variations [see T. J. Crowley, *Quat. Res.* **10**, 275 (1991)].

21. We thank H. Kerp and an anonymous reviewer for comments and the management of Rheinbraun for providing collection facilities. Supported by The Netherlands Foundation for Earth Scientific Research (AWON) with financial aid from The Netherlands Organization for Scientific Research (NWO).

23 December 1992; accepted 29 March 1993

Recent Variability in the Southern Oscillation: Isotopic Results from a Tarawa Atoll Coral

Julia E. Cole,* Richard G. Fairbanks, Glen T. Shen

In the western tropical Pacific, the interannual migration of the Indonesian Low convective system causes changes in rainfall that dominate the regional signature of the El Niño–Southern Oscillation (ENSO) system. A 96-year oxygen isotope record from a Tarawa Atoll coral (1°N, 172°E) reflects regional convective activity through rainfall-induced salinity changes. This monthly resolution record spans twice the length of the local climatological record and provides a history of ENSO variability comparable in quality with those derived from instrumental climate data. Comparison of this coral record with a historical chronology of El Niño events indicates that climate anomalies in coastal South America are occasionally decoupled from Pacific-wide ENSO extremes. Spectral analysis suggests that the distribution of variance in this record has shifted among annual to interannual periods during the present century, concurrent with observed changes in the strength of the Southern Oscillation.

The ENSO system of the tropical Pacific governs interannual variability throughout the tropics and imparts its signature to climate worldwide (*1*). In the western Pacific, ENSO-related changes in the location and intensity of the Indonesian Low convective maximum lead to dramatic shifts in precipitation patterns. At Tarawa Atoll, measurements indicate that intense rainfall alters the salinity of the underlying surface ocean by up to 4 per mil (*2*) and that surface water $\delta^{18}O$ (*3*) varies linearly with salinity. These isotopic changes provide the means by which we can trace the past migrations of the Indonesian Low beyond the historical record with the use of high-

J. E. Cole and R. G. Fairbanks, Lamont-Doherty Earth Observatory, Palisades, NY 10964, and Department of Geological Sciences, Columbia University, New York, NY 10027.
G. T. Shen, School of Oceanography, University of Washington, WB-10, Seattle, WA 98195.

*Present address: Institute for Arctic and Alpine Research, University of Colorado, C.B. 450, Boulder, CO 80309.

resolution $\delta^{18}O$ records from shallow-growing coral skeletons (2, 4, 5). Using this approach, we present a 96-year history of convective rainfall from Tarawa Atoll that doubles the length of the existing instrumental record and yields a record sufficiently long for us to resolve changes in the variance spectrum in this part of the ENSO system.

The interannual shift between extremes of the ENSO system produces coherent sets of oceanographic and climatological anomalies within and beyond the tropical Pacific that have been described by several investigators [for example, (1, 6)]. The cool phase of ENSO is characterized by the zonal Walker circulation, in which easterly winds occur at the surface, the Indonesian Low convective maximum develops over the western Pacific maritime continent, and westerly flow aloft brings dry subsiding air over the eastern and central Pacific. The equatorial easterly winds intensify the upwelling of cool, nutrient-rich waters in the eastern Pacific and transport surface waters westward. This surface flow generates a strong zonal sea-surface temperature (SST) gradient and an eastward slope in sea level. Transition to the warm phase of ENSO occurs when the trade winds relax west of the date line, which allows the western Pacific warm pool to move eastward (7). The Indonesian Low convective maximum migrates to the region near the date line and the equator, upwelling in the eastern Pacific is suppressed, and trade winds remain weak because of the diminished zonal SST gradient. Rainfall patterns across the tropical Pacific shift as the Indonesian Low migrates northeast and convection develops over newly warmed waters.

The present understanding of ENSO has emerged from the instrumental record of tropical Pacific climate, which spans in detail only the past few decades. The few longer records that exist suggest additional complexities, including decoupling of the eastern and western Pacific ENSO components (8), significant decadal variability in ENSO (9, 10), and changes in the overall strength of the Southern Oscillation and its teleconnections (11). These and other observed aspects of this system have yet to be addressed by numerical ENSO models, which have focused on the development of predictive capabilities for large-scale SST changes over time scales of several months to a year. Chemical records from the skeletons of long-lived corals provide the means by which we can extend the length of the climate record beyond the short period of instrumental coverage.

Initial efforts to develop coral paleoclimatic records in the tropical Pacific focused on interannual changes in eastern Pacific upwelling and SSTs (12, 13). In the western Pacific warm pool, changes in SST are small (14), and variability in rainfall and trade winds dominates the interannual climatic signature. Short coral records from sites spanning the Pacific track variability in key features of ENSO, including SST, rainfall, upwelling, and trade wind reversals (5). Tarawa Atoll provides us with a sensitive location from which we can monitor the state of the ENSO system, as intense rainfall accompanies enhanced convection in this region during ENSO warm extremes (4, 15, 16). Over the length of the Tarawa rainfall record (continuous since 1946), cumulative seasonal rainfall greater than 800 mm occurs only during ENSO warm phases, and droughts coincide with ENSO cool phases. Short records from Tarawa indicate that coral $\delta^{18}O$ monitors ENSO-associated rainfall changes (4, 5) and that coralline Mn/Ca ratios provide a site-specif-

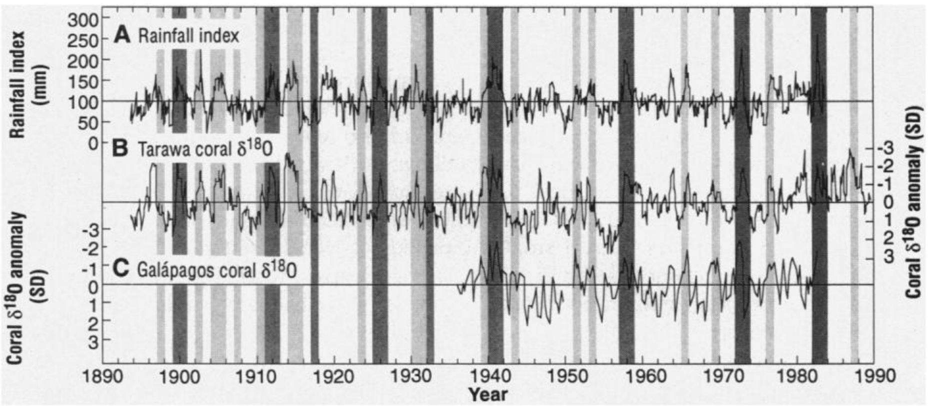

Fig. 1. Comparison of coral $\delta^{18}O$ records with instrumental and historical indices of ENSO. Curve A is an index of central Pacific rainfall (21) with high correlation to ENSO. Curves B and C are coral $\delta^{18}O$ anomaly records from Tarawa Atoll (1°N, 172°E) and the Galápagos (1°S, 89°W), respectively, plotted in units of standard deviation (SD). High correlations between these records are noted in Table 1 and discussed in the text. Shaded bars indicate El Niño events reconstructed from South American historical records (22); darker shading represents strong events, and lighter shading denotes moderate events.

Table 1. Linear, zero-lag correlations between instrumental and coral records of ENSO. In addition to the Tarawa $\delta^{18}O$ record (TARO, 96 years), data include (i) rainfall, SST, and SLP indices from (21) (WRAIN, WSST, and WSOI; 93, 90, and 91 years, respectively); (ii) anomaly indices of Darwin and Tahiti SLP (DSLP and TSLP, 96 years) constructed by subtracting monthly averages from monthly SLP measurements and normalizing (31); (iii) monthly Tarawa rainfall (31) (TRAIN, 44 years); and (iv) a seasonal coral $\delta^{18}O$ anomaly from Punta Pitt, Isla San Cristóbal, Galápagos (13) (GALO, 46 years). Values in parentheses denote that a degree of correlation was built in during index development, as detailed in (21). All correlation coefficients are significant at $P < 0.002$.

	DSLP	TSLP	WSOI	WRAIN	WSST	TRAIN	GALO	TARO
				Monthly				
DSLP	1.00							
TSLP	0.26	1.00						
WRAIN	0.57	0.30		1.00				
WSST	(0.60)	(0.32)		(0.76)	1.00			
TRAIN	0.36	0.27		(0.61)	0.47	1.00		
TARO	0.46	0.27		0.59	0.62	0.39		1.00
				Seasonal				
DSLP	1.00							
TSLP	0.45	1.00						
WSOI	(0.84)	(0.58)	1.00					
WRAIN	0.71	0.44	0.77	1.00				
WSST	(0.77)	(0.46)	(0.81)	(0.84)	1.00			
TRAIN	0.50	0.41	0.57	(0.69)	0.60	1.00		
GALO	0.35	0.25	0.34	0.51	0.47	0.31	1.00	
TARO	0.57	0.37	0.61	0.66	0.67	0.47	0.36	1.00
				Annual				
DSLP	1.00							
TSLP	0.59	1.00						
WSOI	(0.92)	(0.67)	1.00					
WRAIN	0.86	0.58	0.86	1.00				
WSST	(0.89)	(0.58)	(0.92)	(0.92)	1.00			
TRAIN	0.73	0.53	0.88	(0.88)	0.72	1.00		
GALO	0.53	0.50	0.53	0.71	0.76	0.55	1.00	
TARO	0.71	0.49	0.72	0.80	0.78	0.59	0.59	1.00

ic tracer of the trade wind reversals that accompany ENSO warm extremes (17).

In the western equatorial Pacific, the depth of the surface mixed layer is highly variable, averaging 29 ± 26 m. Intense rainfall establishes a relatively fresh surface layer; large variability in mixed-layer thickness reflects the sensitivity of surface stratification to short-term changes in rainfall and winds (18). In tropical ocean regions, intense rainfall has low $\delta^{18}O$ values (19) as a result of isotopic distillation associated with the progressive condensation of vapor during deep convection. At Tarawa, results from an ongoing monitoring program confirm that intense rainfall alters the $\delta^{18}O$ and salinity of the surface mixed layer (2). Shallow-growing corals incorporate this isotopic shift in the $\delta^{18}O$ of their aragonite skeletons (2, 4).

We recovered two cores from a single coral head (genus *Porites*) at a depth of 6.7 m from a forereef site, chosen to reflect open-ocean conditions. We drilled samples for isotopic analysis (20) at 1-mm increments from the complete usable length of each core (mean resolution, 16 samples per year). Ages were determined independently for the two cores on the basis of seasonal $\delta^{13}C$ variability, which is supported by radiometric and density-banding observations of young Tarawa corals (4). We normalized the records, spliced them together using diagnostic density and isotopic patterns, and interpolated them to monthly resolution for statistical analysis.

The monthly resolution record of $\delta^{18}O$ that we obtained (Fig. 1) spans 96 years and doubles the length of the Tarawa rainfall record. Comparison with instrumental and proxy indices of ENSO suggests that the coral $\delta^{18}O$ is sensitive to ENSO variability. Our record also reflects decadal variability in the climate of the western tropical Pacific. The record shows a mean shift to lower $\delta^{18}O$ values (indicating rainier conditions) for the period between 1976 and 1988. The lack of strong positive (dry) extremes during this interval is unlike any earlier time in our record.

To evaluate the quality of the Tarawa coral $\delta^{18}O$ record as a monitor of Pacific climate variability, we compared it with instrumental histories of the ENSO system (Table 1). To compare monthly resolution indices with lower resolution data, we converted the monthly records to seasonal means centered on January, April, July, and October and annual means that span April through March of the following year. We analyzed the period from 1893 to 1989, or the interval within that period in which data exist for a given index. Instrumental records used in these analyses include large-scale indices of tropical Pacific SST, rainfall, and sea-level pressure (SLP) (21); SLP anomalies from Tahiti and Darwin; and rainfall data from Tarawa.

Across monthly, seasonal, and annual resolutions, the Tarawa coral $\delta^{18}O$ record reflects large-scale ENSO variability (Table 1). Coral and instrumental records correlate more strongly when the instrumental data are derived from a network of sites, such as the indices of rainfall and SST; correlations are lower with the inherently noisy single-station rainfall and SLP records. Unlike measurements derived from a single rain gauge, seawater $\delta^{18}O$ changes associated with intense rainfall are broadly integrated in the ocean's surface mixed layer. Correlations between Tarawa coral $\delta^{18}O$ and large-scale ENSO indices compare favorably to correlations between those indices and single-site records such as Tarawa rainfall or Darwin SLP. Thus, the Tarawa coral $\delta^{18}O$ offers an ENSO history comparable in quality and resolution to instrumental climate records over the past century.

Convection and rainfall variability associated with the Indonesian Low form an integral part of most descriptions of ENSO (1). To examine the history of the climatic coupling between the eastern and western equatorial Pacific over this century, we compared the Tarawa $\delta^{18}O$ record with a documentary history of El Niño events from coastal South America (16, 22) and a seasonal $\delta^{18}O$ record from a Galápagos Islands coral (13).

"El Niño event years" have been identified by Quinn and co-workers (22) on the basis of historical evidence from coastal South America for specific climatic, oceanographic, and biological phenomena. During most of these El Niño years, Tarawa $\delta^{18}O$ anomalies exceed 1 SD, although anomaly magnitudes do not always match Quinn's designations. Documented El Niño events in 1907, 1917, 1932, 1943, and 1982 to 1983 have no counterpart in the Tarawa $\delta^{18}O$ record. Except for the extreme event of 1982 and 1983, instrumental data support the lack of ENSO warm-phase anomalies across the Pacific during these times (8, 21). Despite the devastating impact of the 1982 to 1983 anomaly elsewhere (23), the Tarawa rainfall record indicates near-normal conditions; the coral $\delta^{18}O$ record monitors this period accurately. Out-

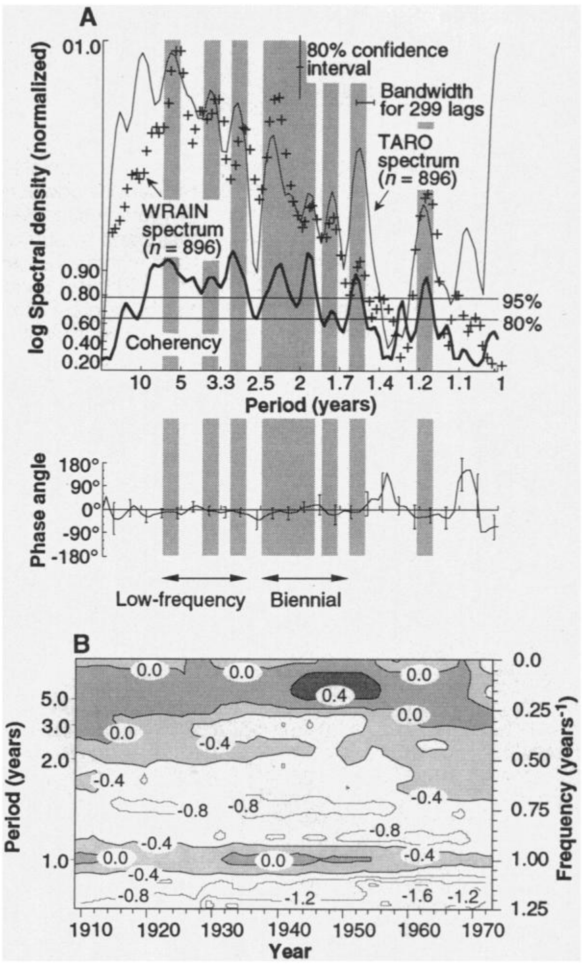

Fig. 2. (**A**) Results of cross-spectral analysis between the Tarawa coral record and a rainfall index that monitors ENSO variability (21). The upper panel plots the variance spectra [as normalized log (spectral density), where spectral density equals variance divided by frequency] of the coral $\delta^{18}O$ record (thin line) and of the rainfall index (+) as well as the coherency of these signals (heavy line). The lower panel indicates the phasing of the two time series. Coherent variance peaks emerge at interannual periods centered on 5.6, 3.6, 3.0, and 1.9 to 2.4 years; at these periods, coherency values ≥0.9 indicate that over 80% of the variance in these frequency bands is linearly correlated between these time series. Similar analyses using ENSO indices derived from SST and SLP variations show coherent variance peaks over the same frequency bands, with comparable coherencies (2). (**B**) Evolutionary spectrum of variability in the Tarawa coral $\delta^{18}O$ record. This figure maps the changing concentrations of variance (in units of log spectral density) in the Tarawa $\delta^{18}O$ record throughout the present century from spectral analysis (26) of overlapping 30-year intervals of monthly $\delta^{18}O$ data, offset by 2 years. Results are plotted against the midpoint of the analysis interval. Shading denotes relatively higher concentrations of variance. The error is 0.36 above and 0.22 below the values. Overall, this figure suggests a change in the behavior of ENSO between about 1930 and 1950, with greater power at 5- to 6-year and annual periods and reduced power at 3-year periods.

going long-wave radiation measurements indicate that the convective maximum bypassed Tarawa and moved far east of the date line in 1982 (*24*). In 1946 to 1947, 1963, and 1980, the Tarawa $\delta^{18}O$ record suggests unusually rainy periods at Tarawa that have no counterparts in Quinn's El Niño chronology. These periods have been previously noted as times of weak ENSO warm-phase conditions (*16, 25*). Our comparison suggests a tendency for equatorial Pacific anomalies to have at least a small impact along the South American coast, whereas coastal anomalies do not always reflect unusual conditions across the equatorial Pacific.

Comparison of the $\delta^{18}O$ anomaly records from Galápagos (*13*) and Tarawa corals reveals that these records generally match well. Years of ENSO warm extremes ($\geq$1 SD below the mean) are consistent between both records. However, positive (cool and dry) $\delta^{18}O$ anomalies recur more frequently in the Galápagos record than in the Tarawa record. The high frequency of positive $\delta^{18}O$ extremes in the Galápagos coral record is consistent with the record of SSTs from Puerto Chicama, Peru, but ENSO cool extremes appear less frequently in instrumental records from central and western Pacific sites.

Cross-spectral analysis (*26, 27*) indicates that the Tarawa $\delta^{18}O$ record is consistently and significantly coherent with instrumental ENSO indices (*21*) over periods centered at 2.3, 3.0, 3.6, and 5.8 years (Fig. 2A). At these periods, 75 to 85% of $\delta^{18}O$ variance correlates linearly to ENSO. Our results agree with earlier studies suggesting that ENSO-related climate variables are characterized by broad concentrations of variance across annual, biennial, and low-frequency (3- to 7-year) periods (*28*), although the length of our record enables more detailed resolution of specific periods. The periods that characterize ENSO variability in the Tarawa record also emerge in records of east African rainfall (*29*), where strong ENSO teleconnections occur (*6*).

To evaluate changes in the relative contributions of dominant frequency components over the past 96 years, we applied spectral analysis to overlapping 30-year intervals of the Tarawa $\delta^{18}O$ record, offset by 2 years (Fig. 2B). This evolutionary spectrum shows significant changes in concentrations of variance at periods coherent with ENSO (Fig. 2A). Notable features include the decline in power at the 3-year period from 1930 to 1952, the maximum in the low-frequency component between 1940 and 1955, and the recent weakening of the annual cycle from a maximum in strength between 1930 and 1950. Taken together, these results suggest that the pulse of rainfall variability at Tarawa between about 1930 and 1950 differed from that of preceding or subsequent periods.

These results suggest a shift in the pulse of ENSO that may relate to large-scale patterns of climatic correlation and teleconnection. Between 1930 and 1965, a general weakening of the Southern Oscillation is suggested by reduced correlation of climatic anomalies within and beyond the tropical Pacific (*11*). The Southern Oscillation was apparently stronger from 1900 to 1930 and since 1965, periods when the 3-year component of the Tarawa coral record is most intense and the annual component weakest. A strong annual cycle between 1930 and 1950 may reflect increased seasonal influence of either the southeast Asian monsoon or the eastern Pacific cold tongue. Deciphering these changes requires additional coral measurements [for example, Sr/Ca ratios (*30*)]. Longer records and additional sites are needed for the evaluation of the full range of natural variability in ENSO, including spectral evolution, sensitivity to extratropical changes, and the possibility that recent climate shifts may be unprecedented.

REFERENCES AND NOTES

1. M. A. Cane, *Annu. Rev. Earth Planet. Sci.* **14**, 43 (1986); D. B. Enfield, *Rev. Geophys.* **27**, 159 (1989); S. G. H. Philander, *El Niño, La Niña, and the Southern Oscillation* (Academic Press, New York, 1990).
2. J. E. Cole, thesis, Columbia University (1992).
3. The oxygen isotopic content of a sample is expressed in parts per thousand (per mil) as $\delta^{18}O$, where the δ notation is defined in terms of the isotopic ratio R ($^{18}O/^{16}O$) in the sample relative to a standard: $\delta = [(R_{sample} - R_{standard})/R_{standard}] \times 1000$. For coralline aragonite $\delta^{18}O$, the conventional reference standard is the Pee Dee belemnite, or PDB.
4. J. E. Cole and R. G. Fairbanks, *Paleoceanography* **5**, 669 (1990).
5. J. E. Cole, G. T. Shen, R. G. Fairbanks, M. Moore, in *El Niño: Historical and Paleoclimatic Aspects of the Southern Oscillation*, H. F. Diaz and V. Markgraf, Eds. (Cambridge Univ. Press, Cambridge, 1992), pp. 349–375.
6. C. F. Ropelewski and M. S. Halpert, *Mon. Weather Rev.* **115**, 1606 (1987); M. S. Halpert and C. F. Ropelewski, *J. Clim.* **5**, 577 (1992).
7. R. Lukas, S. P. Hayes, K. Wyrtki, *J. Geophys. Res.* **89**, 10425 (1984); M. J. McPhaden and J. Picaut, *Science* **250**, 1385 (1990).
8. C. Deser and J. M. Wallace, *J. Geophys. Res.* **92**, 14189 (1987).
9. N. S. Cooper, K. D. B. Whysall, G. R. Bigg, *Int. J. Climatol.* **9**, 221 (1989).
10. K. E. Trenberth, *Bull. Am. Meteorol. Soc.* **71**, 988 (1990).
11. ______ and D. J. Shea, *Mon. Weather Rev.* **115**, 3078 (1987); W. P. Elliott and J. K. Angell, *J. Clim.* **1**, 729 (1988); J. Michaelsen and L. G. Thompson, in (*5*), pp. 323–348.
12. E. R. M. Druffel, in *The Carbon Cycle and Atmospheric CO_2: Natural Variations Archean to Present*, W. S. Broecker and E. T. Sundquist, Eds. (American Geophysical Union, Washington, DC, 1985), p. 111; R. B. Dunbar, G. M. Wellington, M. W. Colgan, P. W. Glynn, in *Proceedings of the Seventh Annual Pacific Climate (PACLIM) Workshop*, J. L. Betancourt, Ed. (California Department of Water Resources, Sacramento, 1991), pp. 183–198; G. T. Shen *et al.*, *Coral Reefs* **10**, 91 (1991).
13. G. T. Shen *et al.*, *Paleoceanography* **7**, 563 (1992).
14. S. Levitus, *Climatological Atlas of the World Ocean* (National Oceanic and Atmospheric Administration, Washington, DC, 1982); E. M. Rasmusson and T. H. Carpenter, *Mon. Weather Rev.* **110**, 354 (1982).
15. J. D. Horel and J. M. Wallace, *Mon. Weather Rev.* **109**, 813 (1981).
16. W. H. Quinn, D. O. Zopf, K. S. Short, K. T. W. Yang, *Fish. Res. Bull.* **76**, 663 (1978).
17. G. T. Shen, L. J. Linn, T. M. Campbell, J. E. Cole, R. G. Fairbanks, *J. Geophys. Res.* **97**, 12689 (1992).
18. E. Lindstrom *et al.*, *Nature* **330**, 533 (1987); R. Lukas and E. Lindstrom, *J. Geophys. Res.* **96**, 3343 (1991); P. J. Webster and R. Lukas, *Bull. Am. Meteorol. Soc.* **73**, 1377 (1992).
19. W. Dansgaard, *Tellus* **16**, 436 (1964); Y. Yurtsever and J. R. Gat, in *Stable Isotope Hydrology: Deuterium and Oxygen-18 in the Water Cycle*, J. R. Gat, Ed. (International Atomic Energy Agency, Vienna, 1981), pp. 103–142.
20. Samples were taken along the axis of maximum growth and analyzed, without pretreatment, on a Finnigan MAT 251 mass spectrometer with an automated Carousel-48 carbonate device. Carbonate standards indicate precision of better than $\pm$0.08 per mil $\delta^{18}O$ and $\pm$0.04 per mil $\delta^{13}C$. We obtained excellent replication of the isotopic signal in several contexts, including in regions of overlap between cores and in slabs where two transects were sampled.
21. P. B. Wright, *Int. J. Climatol.* **9**, 33 (1989).
22. W. H. Quinn, V. T. Neal, S. E. Antunez de Mayolo, *J. Geophys. Res.* **92**, 14449 (1987); W. H. Quinn and V. T. Neal, in *Climate Since A.D. 1500*, R. S. Bradley and P. D. Jones, Eds. (Routledge, London, 1992), p. 623.
23. P. W. Glynn, Ed., *Global Ecological Consequences of the 1982–83 El Niño-Southern Oscillation* (Elsevier, New York, 1990).
24. E. M. Rasmusson and J. M. Wallace, *Science* **222**, 1195 (1983).
25. J.-R. Donguy and A. Dessier, *Mon. Weather Rev.* **111**, 2136 (1983).
26. Spectral and cross-spectral analyses were performed with the use of the ARAND package for Macintosh computers, which was provided by investigators at Brown University (J. Imbrie, W. Prell, and P. Howell). These methods are based on the Blackman-Tukey technique. G. M. Jenkins and D. G. Watts, *Spectral Analysis and Its Applications* (Holden-Day, Oakland, CA, 1968).
27. J. Imbrie, A. McIntyre, A. Mix, in *Understanding Climate Change*, A. L. Berger, R. E. Dickinson, J. W. Kidson, Eds. (American Geophysical Union, Washington, DC, 1989), p. 121.
28. E. M. Rasmusson, X. Wang, C. Ropelewski, *J. Mar. Syst.* **1**, 71 (1990); T. P. Barnett, *J. Clim.* **4**, 269 (1991); C. F. Ropelewski, M. S. Halpert, X. Wang, *ibid.* **5**, 594 (1992).
29. H. Rodhe and H. Virji, *Mon. Weather Rev.* **104**, 307 (1976); S. E. Nicholson, in (*27*), p. 79.
30. The Sr/Ca ratio measurements appear to provide a pure temperature signal in coralline aragonite; J. W. Beck *et al.*, *Science* **257**, 644 (1992).
31. Monthly records of SLP from Darwin and Tahiti were supplied by C. Ropelewski of the Climate Analysis Center, National Oceanic and Atmospheric Administration (NOAA). Tarawa rainfall data were provided by the Fisheries Division of the Kiribati Ministry for Natural Resources Development.

32. Supported by the Paleoclimatology Program of NOAA (NA16-RC-0079-01), the National Science Foundation (ATM-88-15193), and the Climate Center of Lamont-Doherty Earth Observatory (LDEO). We thank the Fisheries Division of the Kiribati Ministry of Natural Resources Development for its support, especially J. Uan for providing water samples. On Tarawa, W. Schutz and V. Stinnet provided logistical assistance and R. Espinosa assisted in coral drilling. The manuscript benefited from comments by J. Overpeck, K. Wolter, and anonymous reviewers and J. Imbrie provided guidance on the frequency-domain analyses. This is LDEO contribution 5060.

15 January 1993; accepted 25 March 1993